**Magnesium Technology 2014**
*Edited by: Martyn Alderman, Michele V. Manuel, Norbert Hort, and Neale R. Neelameggham*
***TMS (The Minerals, Metals & Materials Society), 2014***

# Significant Precipitation Strengthening in Extruded Mg-Sn-Zn Alloys

T.T. Sasaki[1], F.R. Elsayed[1, 2], T. Nakata[3], S. Kamado[3], T. Ohkubo[1] and K. Hono[1]
[1] National Institute for Materials Science, 1-2-1 Sengen, Tsukuba, 305-0047, Japan
[2] Graduate School of Pure and Applied Science, The University of Tsukuba, 305-0001 Japan
[3] Nagaoka University of Technology, 1603-1, Kamitomiokacho, Nagaoka, 940-2188, Japan

Keywords: Mg-Sn-Zn alloy, precipitation hardening, extrusion

## Abstract

Mg–5.4Sn-4.2Zn-2.1Al-0.2Mn (TZAM5420) and Mg–5.4Sn-4.2Zn-2.1Al-0.2Mn-0.1Na (TZAM5420-0.1Na) alloys were extruded at various ram speeds, and the effect of the ram speed and T6 treatment on the strength was investigated. Particularly, the TZAM5420-0.1Na alloy extruded at 5 mm/s exhibited a yield strength of 334 MPa after the T6 treatment, which is more than 170 MPa higher than that of the as-extruded alloy. The high strength of the T6 aged TZAM5420-0.1Na alloy is attributed to the uniform dispersion of the fine precipitates and suppressed grain growth during the solution treatment.

## Introduction

There are growing research interests in the development of high strength wrought magnesium alloys applicable to transportation vehicles and aircrafts due to the strong demands for the reduction of $CO_2$ emission by their weight reduction. Since commercially available wrought Mg-Zn-Zr (ZK) and Mg-Al-Zn (AZ) alloy families have shown only moderate precipitation hardening responses by T5 treatment **[1]**, the precipitation hardening has not been paid much attention as a method to strengthen the wrought alloys. However, a number of renewed efforts have been made, and the precipitation hardening response was substantially enhanced by macro- and micro-alloying in the existing precipitation hardenable alloys such as Mg-Zn, Mg-Al, Mg-Ca, Mg-Sn, and Mg-RE (RE: rare-earth element) alloys **[2]**. Recent work on the twin-roll cast and hot rolled ZK60 alloy microalloyed with Ag and Ca exhibited excellent formability after the solution treatment, and high strength over 300 MPa after T6 treatment **[3]**, making the precipitation hardenable alloys promising as the wrought alloys.

The Mg-Sn based extruded alloy also exhibits the high strength of over 300 MPa in the as-extruded condition **[4-6]**. To achieve such high strength, the sample needed to form fine-grained structure by extruding at an unrealistically slow speed from the viewpoint of practical applications. Since the slow speed extrusion results in the increase in the production cost to hinder the application, we need to explore the industrially viable processing route as well as achieving the high strength. While the extrusion at high speed can reduce the production cost, the strength of the as-extruded sample decreases with increasing the extrusion speed mainly because of microstructure coarsening **[7, 8]**. Unlike the Mg-Zn-Zr (ZK) and Mg-Al-Zn (AZ) commercial alloys, T5 and T6 treatments do not work to further strengthen the Mg-Sn based extruded alloy **[9, 10]**. With this background, we have developed a Mg-5.4Sn-4.3Zn-2.0Al (wt.%) alloy containing trace amount of Mn and Na, in which the composition is optimized to exhibit high age hardening response. The sample exhibits the strength increase of more than 100 MPa by T6 treatment, and shows high strength up to 350 MPa **[11]**. In this work, we have extruded the Mg-1.2Sn-1.7Zn-2.0Al(-0.1Na) (at.%) alloy at various extrusion speeds, and investigated the effect of T6 aging on the mechanical property.

## Experimental Procedure

Alloy ingots with nominal compositions of Mg-5.4Sn-4.2Zn-2.1Al-0.2Mn and Mg-5.4Sn-4.2Zn-2.1Al-0.2Mn-0.1Na in wt.% were prepared by induction melting using steel crucibles under an Ar atmosphere and by casting into iron molds. Table 1 summarizes the nomenclatures and compositions in both at.% and wt.%. The ingots were homoogenized at 350 °C for 24 h followed by 450 °C heat treatment for 24 h in an Ar-atmosphere followed by water quenching. The homogenized samples were then extruded at 300 °C with the ram speeds of 0.1, 2, 5 mm/s and extrusion ratio of 20. The extruded samples were solution treated at 450 °C for 15 min in an electric furnace and subjected to T6 aging at 160 °C in an oil bath.

The age hardening responses were measured by the Vickers hardness measurements under a load of 500 g. Mechanical properties of the as-extruded and peak aged samples were evaluated by tensile tests at an initial strain rate of $1.0\times10^{-3}$ $s^{-1}$ using the round bar sample with the gauge length and diameter of 22 and 4 mm, respectively.

Microstructure characterization was performed by scanning electron microscope (SEM) and transmission electron microscope (TEM). Electron backscattered diffraction (EBSD) analyses were done using a field emission gun-SEM, Carl Zeiss Cross Beam 1540EsB, equipped with a HKL EBSD system and CHANNEL 5 software. TEM observation was carried out using FEI Tecnai T20 TEM. Thins foils for the TEM observation were prepared by punching 3 mm diameter discs, mechanical polishing and ion-milling using a Gatan Precision Ion Polishing System (PIPS).

Table 1: Chemical compositions and nomenclatures of the samples prepared in this work

| Nomenclature | Composition | |
|---|---|---|
| | at.% | wt.% |
| TZAM5420 | Mg-1.2Sn-1.7Zn-2.0Al-0.1Mn | Mg-5.4Sn-4.2Zn-2.1Al-0.2Mn |
| TZAM5420-0.1Na | Mg-1.2Sn-1.7Zn-2.0Al-0.1Mn-0.1Na | Mg-5.4Sn-4.2Zn-2.1Al-0.2Mn-0.1Na |

## Results and Discussions

**Figure 1 (a)** shows the tensile stress-strain curves of as-extruded TZAM5420 and TZAM5420-0.1Na alloys. Table 2 summarizes the tensile yield strength, $\sigma_{ys}$, ultimate tensile strength, $\sigma_{UTS}$, and elongation to failure, $\varepsilon$, obtained from the stress-strain curves. The tensile yield strength, $\sigma_{ys}$, decreases with increasing the extrusion speed in both TZAM5420 and TZAM5420-0.1Na alloys. The $\sigma_{ys}$ of the TZAM5420 alloy decreases from 222 to 163 MPa with increasing the ram speed from 0.1 to 5 mm/s while the elongation to failure increases from 0.18 to 0.23. The $\sigma_{ys}$ of the TZAM5420-0.1Na alloy exhibits higher strength but lower elongation to failure compared to the TZAM5420 alloy. The $\sigma_{ys}$ of the TZAM5420-0.1Na alloy also decreases from 303 to 168 MPa with increasing the ram speed from 0.1 to 5 mm/s while the elongation to failure increases from 0.07 to 0.18.

Table 2: Tensile properties of as-extruded samples

| Sample | Ram Speed | $\sigma_{ys}$, MPa | $\sigma_{UTS}$, MPa | ε |
|---|---|---|---|---|
| TZAM5420 | 0.1 mm/s | 222 | 332 | 0.18 |
| | 2 mm/s | 182 | 324 | 0.23 |
| | 5 mm/s | 163 | 313 | 0.23 |
| TZAM5420-0.1Na | 0.1 mm/s | 303 | 352 | 0.07 |
| | 2 mm/s | 243 | 324 | 0.09 |
| | 5 mm/s | 168 | 287 | 0.18 |

TZAM5420 and TZAM5420-0.1Na alloys extruded at 5 mm/s were selected to investigate the effect of T6 treatment on the mechanical properties. Figure 1 (b) shows the variations in Vickers hardness of the TZAM5420 and TZAM5420-0.1Na alloys extruded at 5 mm/s as a function of aging time during aging at 160 °C. After the solution treatment, the hardness values of both TZAM5420 and TZAM5420-0.1Na alloys decrease to 49.0 and 50.8 VHN, respectively. The hardness of the TZAM5420 alloy starts to increase significantly after 16 h, and reaches the peak hardness of 73.4 VHN at 300 h. The TZAM5420-0.1Na alloy exhibits the significant hardness increase after 3 h of aging, and reaches the peak hardness of 93.1 VHN at 100 h. Interestingly, the samples are not overaged at least until 1600 h.

Figure 1 (c) shows the stress-strain curves of the TZAM5420 and TZAM5420-0.1Na alloys extruded at 5 mm/s in the as-extruded and peak aged conditions. Table 3 summarizes the tensile yield strength, $\sigma_{ys}$, ultimate tensile strength, $\sigma_{UTS}$, and elongation to failure, $\varepsilon$, obtained from the stress-strain curves. By the T6 aging, the yield strength increases at the expense of the elongation to failure. The $\sigma_{ys}$ of the TZAM5420 alloy slightly increases from 163 to 207 MPa by T6 treatment while ε decreased to 0.07. Surprisingly, the $\sigma_{ys}$ of the TZAM5420-0.1Na alloy significantly increases to 335 MPa from 168 MPa by T6 treatment although the $\varepsilon$ is significantly decreased to 0.03.

Table 3: Tensile properties of TZAM5420 and TZAM5420-0.1Na alloys extruded at 5 mms in as-extruded and peak aged conditions

| Sample | Ram Speed | $\sigma_{ys}$, MPa | $\sigma_{UTS}$, MPa | ε |
|---|---|---|---|---|
| TZAM5420 | As-Ext. | 163 | 313 | 0.23 |
| | T6 | 207 | 282 | 0.07 |
| TZAM5420-0.1Na | As-Ext. | 168 | 287 | 0.18 |
| | T6 | 335 | 356 | 0.03 |

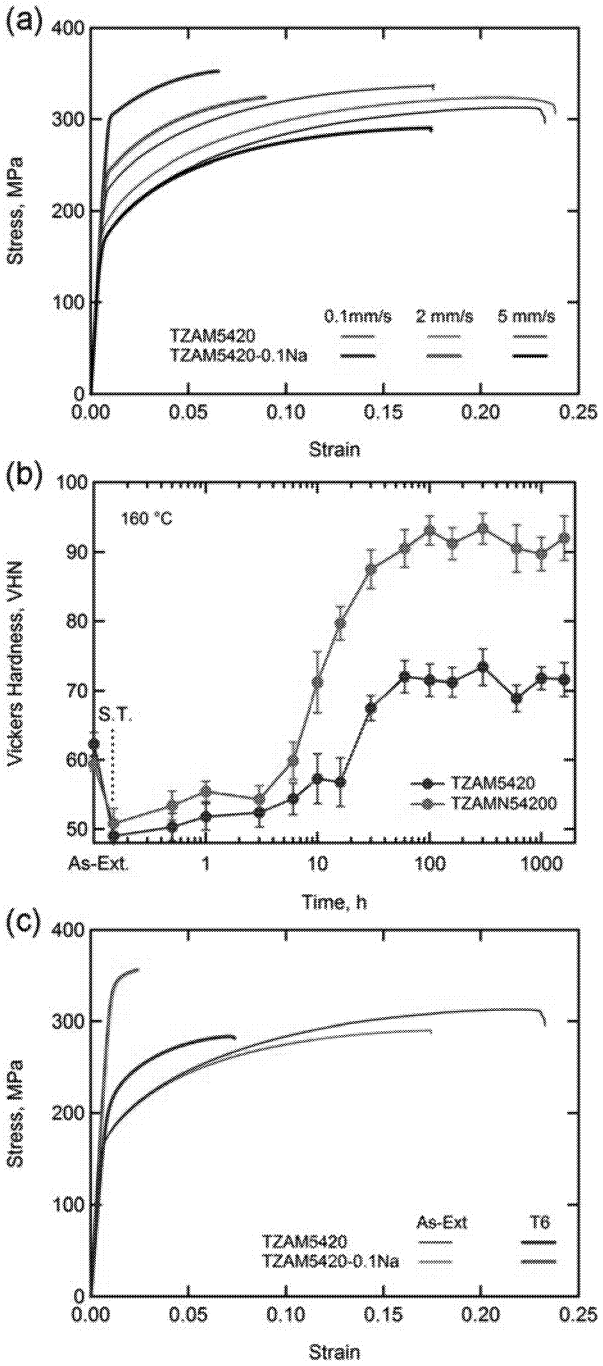


Figure 1: (a) Engineering stress-strain curves of Mg-5.4Sn-4.2Zn-2.1Al-0.1Mn (TZAM5420) and Mg-5.4Sn-4.2Zn-2.1Al-0.1Mn-0.1Na (TZAM5420-0.1Na) alloys extruded at different ram speeds. (b) Variations in Vickers hardness of TZAM5420 and TZAM5420-0.1Na alloys as a function of aging time during aging at 160 °C. (c) Engineering stress-strain curves of TZAM5420 and TZAM5420-0.1Na alloys extruded at 5 mm/s in as-extruded and peak aged conditions.

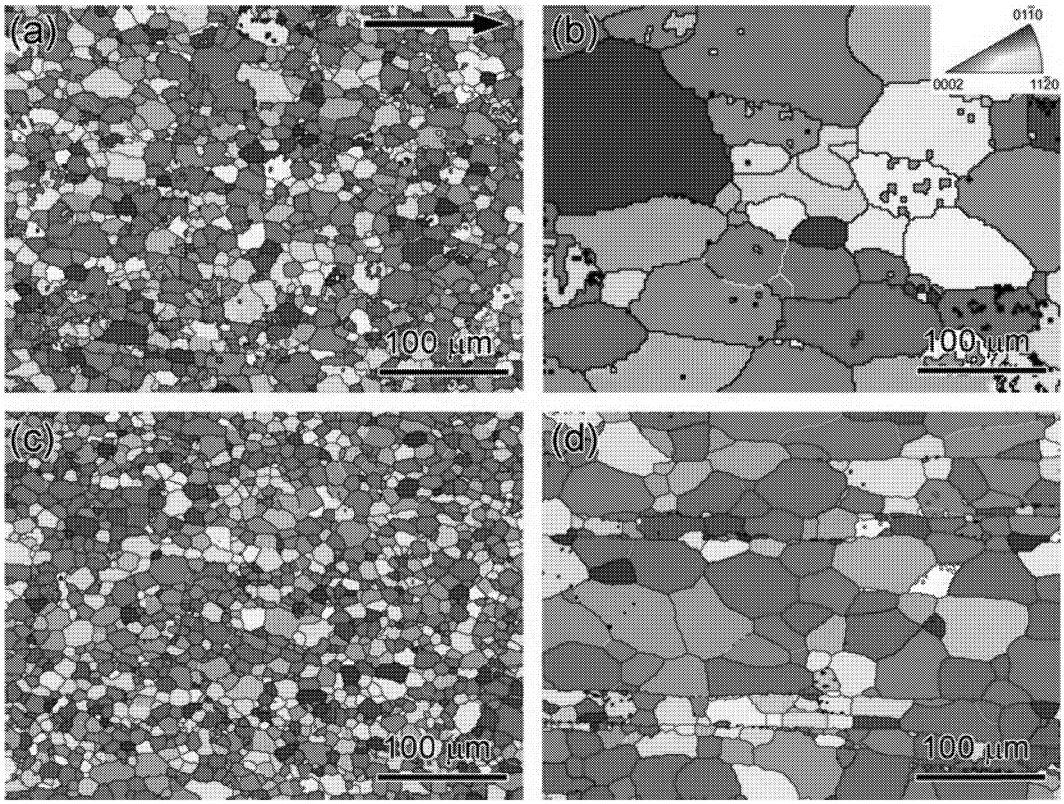


Figure 2: Inverse pole figure maps obtained from (a) as-extruded and (b) solution treated TZAM5420 alloys, and (c) as-extruded and (d) solution treated TZAM5420-0.1Na alloys. Note that the arrow in (a) shows the extrusion direction.

Figure 2 (a) thorough (d) show inverse pole figure (IPF) maps obtained from the (a) as-extruded and (b) solution treated TZAM5420 alloys, and the (c) as-extruded and (d) solution treated TZAM5420-0.1Na alloys. The as-extruded samples consist of relatively fine recrystallized grains with equi-axed shape, and their mean grain sizes are 13.6 and 10.8 μm for the TZAM5420 and TZAM5420-0.1Na alloys. The TZAM5420-0.1Na alloy shows slightly finer grain structure compared to the TZAM5420 alloy. While the grains are coarsened upon the solution treatment at 450 °C, the grain growth is rather suppressed in the TZAM5420-0.1Na alloy as shown in Fig. 2 (b) and (d); the grain size of the solution treated TZAM5420 and TZAM5420-0.1Na alloys is 58.6 and 32.1 μm, respectively.

Figure 3 show pole figures analyzed from the IPF maps in Fig. 2. Due to low counting statistics of the grains for the solution treated TZAM5420 alloy, the analysis was done for the as-extruded TZAM5420 and TZAM5420-0.1Na alloys and solution treated TZAM5420-0.1Na alloy. As shown in Fig. 3 (a) and (b), the as-extruded samples exhibit the textured feature, which is typically observed in the extruded magnesium alloys; the (0001) plane of the magnesium matrix is aligned normal to the extrusion direction. In addition, since there is no significant difference in the maximum intensities between the as-extruded TZAM5420 and TZAM5420-0.1Na alloy, these samples show the similar textured feature. Although the number of grains analyzed was smaller compared to the as-extruded samples, the (0001) plane of the grains is still aligned normal to the extrusion direction after the solution treatment indicating that the extruded texture is maintained after the solution treatment, Fig. 3 (c).

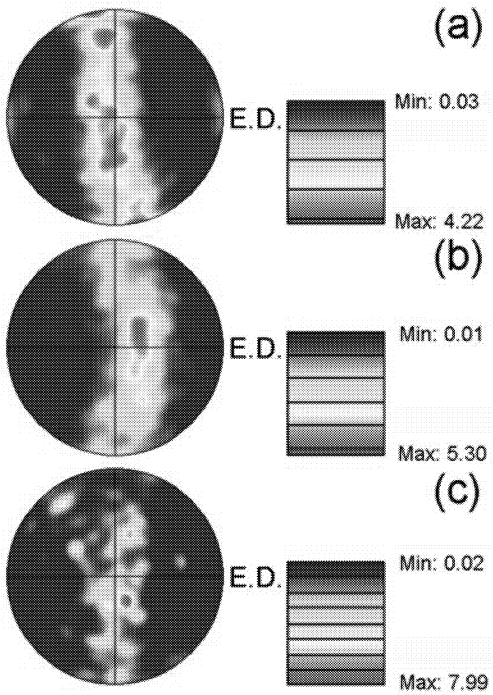


Figure 3: (0001) pole figures obtained from (a) as-extruded TZAM5420, (b) as-extruded TZAM5420-0.1Na, and (c) solution treated TZAM5420-0.1Na alloys.

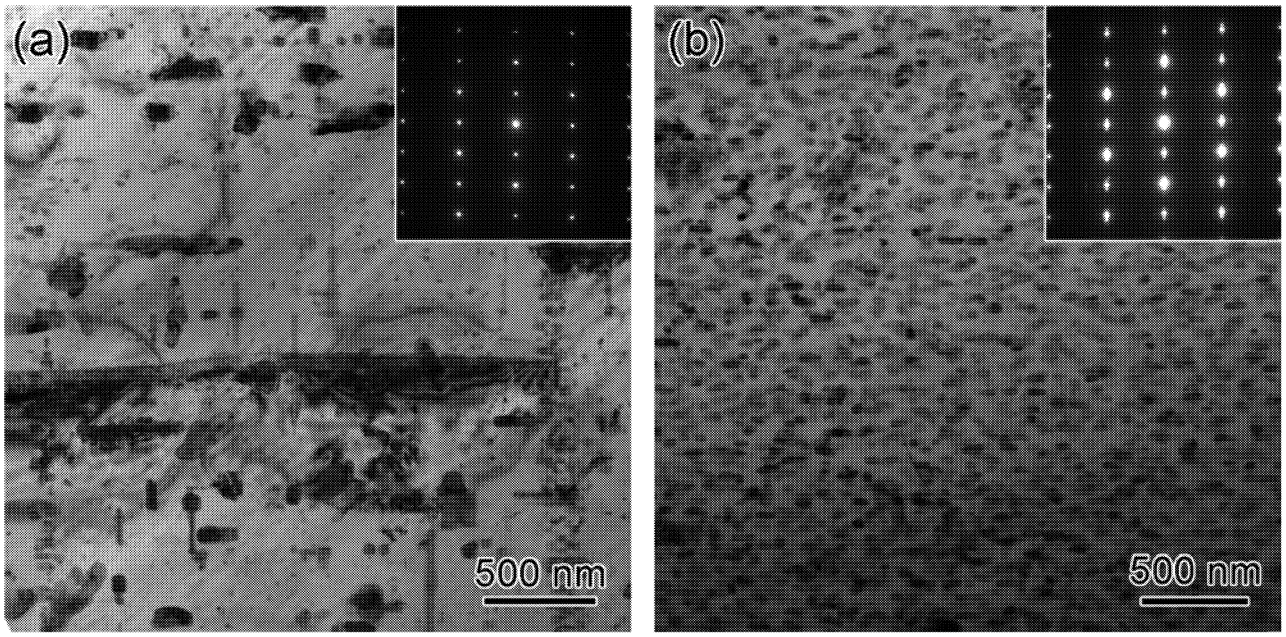


Figure 4: Bright field TEM images of peak aged (a) TZAM5420 and (b) TZAM5420-0.1Na alloys observed from the zone axis of $[11\bar{2}0]$.

Figure 4 (a) and (b) show the bright field TEM image obtained from the peak aged TZAM5420 and TZAM5420-0.1Na alloys taken from the zone axis of $[11\bar{2}0]$. In the TZAM5420 alloy, three types of precipitates are observed; fine cuboidal precipitates, rod-like precipitates and lath-shaped precipitates. Fine cuboidal precipitates could be identified as $\beta_2'$ phase in the previous reports **[13, 14]**. The rod-like precipitates growing along [0001] direction are $\beta_1'$ phase **[13, 14]**. The coarse lath shaped precipitates forms on the (0001) plane of the magnesium matrix, and they are identified as $Mg_2Sn$ phase **[13]**. These precipitates are heterogeneously dispersed within the matrix. In the TZAM5420-0.1Na alloy, the precipitates mainly form on the (0001) plane of the magnesium matrix, and have the length of 33.9±6.29 nm. They are much finer and uniformly dispersed compared to the ones in the peak aged TZAM5420 alloy.

In this work, we have investigated the effect of the extrusion speed and T6 treatment on the strength of the TZAM5420 and TZAM5420-0.1Na alloys. As shown in Fig. 1 (a), the strength of the as-extruded sample decreased with increasing the extrusion speed. The strength degradation due to the increased extrusion speed is attributed to the grain coarsening since the grain size of the TZAM5420 and TZAM5420-0.1Na alloys extruded at 5 mm/s is 13.6 and 10.8 μm, which is coarser than those extruded at 2 mm/s, 4.9 and 2.5 μm **[11]**, Fig. 2 (a) and (c). The increase in the extrusion speed resulted in the generation of larger amount frictional heat, which caused the grain coarsening during the extrusion at higher speed **[10, 11]**.

The TZAM5420 and TZAM5420-0.1Na alloys extruded at 5 mm/s exhibited the fully recrystallized grain structure in the as-extruded condition, Fig. 2 (a) and (c), while the ones extruded at 2 mm/s exhibited bimodal grain structure consisting of coarse unrecrystallized grains and fine recrystallized grains **[11]**. Since the unrecrystallized grains exhibit strongly textured feature, and store high density of dislocations, they are expected to contribute to the strengthening. Therefore, the absence of the unrecrystallized grain might have also caused the strength degradation.

The peak aged TZAM5420-0.1Na alloy exhibited a high yield strength of 335 MPa while the yield strength of the peak aged TZAM5420 alloy was only 207 MPa, Fig. 1 (c). This is mainly because of uniform dispersion of the fine precipitates in the TZAM5420-0.1Na alloy compared to the TZAM5420 alloy by T6 aging, Fig. 4 (a) and (b). The refinement of the precipitates is attributed to the formation of Sn-Na co-clusters, which provide the heterogeneous nucleation sites of the $Mg_2Sn$ precipitates **[15]**. In addition, the solution treated TZAM5420-0.1Na alloy exhibited finer grain structure compared to the TZAM5420 alloy, Fig. 2 (b) and (d). Since Na segregates at the grain boundaries **[11]**, the segregation of Na suppressed the grain growth.

The yield strength of the peak aged TZAM5420-0.1Na alloy extruded at 5 mm/s is mostly equivalent to that extruded at 2 mm/s, 343 MPa **[11]**. This means that the extrusion speed can be increased as fast as possible, and the strength can be increased by the precipitation hardening. The development of industrially viable heat treatable wrought magnesium alloy, further acceleration of age hardening response would be needed as well as the excellent extrudability,.

## Summary

In this work, TZAM5420 and TZAM5420-0.1Na alloys were extruded at various ram speeds. The yield strength decreased with increasing the ram speed because of grain coarsening. Upon the T6 treatment, TZAM5420-0.1Na alloy showed significantly higher age hardening response, and exhibited higher yield strength of 334 MPa while the peak aged TZAM5420 alloy exhibited a yield strength of only 207 MPa. The high strength of the TZAM5420-0.1Na alloy is attributed to the uniform dispersion of the fine precipitates and the suppressed grain growth during the solution treatment.

**Acknowledgement**

This work was supported by JSPS, Graint-in-Aid for Young Scientists (B), 24760605, Grant-in-Aid for Scientific Research on Innovative Area, "Bulk Nano Metal", and JST, Advanced Low Carbon Technology Research and Development Program, (ALCA).

**References**

[1] M.M. Avedesian, H. Baker, eds. Magnesium and Magnesium Alloys ASM Specialty Handbook. ASM International, Materials Park, OH, 1999.

[2] J.F. Nie, "Precipitation and Hardening in Magnesium Alloys" *Metallurgical and Materials Transactions A*, 43 (11) (2012) 3891-3939.

[3] C.L. Mendis, K.Oh-ishi, Y. Kawamura, T. Honma, S. Kamado, K. Hono, "Precipitation-hardenable Mg-2.4Zn-0.1Zn-0.1Ca-0.16 Zr (at.%) alloys," *Acta Materialia*, 57 (3) (2009) 749-760.

[4] T.T. Sasaki, K. Yamamoto, T. Honma, S. Kamado, K. Hono, "A high-strength Mg–Sn–Zn–Al alloy extruded at low temperature", *Scripta Materialia*, *59* (10) (2008) 1111-1114.

[5] H.T. Son, J.B. Lee, H.G. Jeong, T.J. Konno, "Effects of Al and Zn additions on mechanical properties and precipitation behaviors of Mg–Sn alloy system", *Materials Letters, 65* (12) (2011) 1966-1969.

[6] Y.K. Kim, S.W. Sohn, Do H. Kim, W.T. Kim, D.H. Kim, "Role of icosahedral phase in enhancing the strength of Mg-Sn-Zn-Al alloy", *Journal of Alloys and Compounds, 549* (5) (2013) 46-50.

[7] W.L. Cheng, S.S. Park, B.S. You, B.H. Koo, "Microstructure and mechanical properties of binary Mg–Sn alloys subjected to indirect extrusion", Mater. Sci. Eng. A, 527 (18-19) (2010) 4650-4653.

[8] F.R. Elsayed, T.T. Sasaki, T. Ohkubo, H. Takahashi, S.W. Xu, S. Kamado, K. Hono, "Effect of extrusion conditions on microstructure and mechanical properties of microalloyed Mg-Sn-Al-Zn alloys", *Materials Science and Engineering A*, In Press.

[9] J.R. TerBush, M. Setty, N. Stanford, M.R. Barnett, A.J. Morton, J.F. Nie, Proceedings of 9th International Conference on Magnesium Alloys and their Applications, pp. 579-586.

[10] T.T. Sasaki, , J.D. Ju, K. Hono, K.S. Shin, "Heat-treatable Mg–Sn–Zn wrought alloy", *Scripta Materialia*, 61 (1) (2009) 80-83.

[11] T.T. Sasaki, F.R. Elsayed, H. Takahashi, T. Nakata, T. Ohkubo, S. Kamado, K. Hono, "Significant Precipitation Strengthening of Extruded Mg-5.4Sn-4.2Zn-2.0Al Alloy Microalloyed with Na and Mn", *Under Review.*

[12] N. Stanford, J.R. TerBush, M. Setty, M.R. Barnett, Metallurgical and Materials Transactions A 44A (6) (2013) 2466 – 2469.

[13] T. Sasaki, T. Ohkubo and K. Hono, *Magnesium Technology 2012*, Eds by S.N. Mathaudhu, W.H. Sillekens, N.R. Neelameggham, The Minerals, Metals & Materials Society (TMS), 2012, pp. 181-185.

[14] K. Oh-ishi, K. Hono, K.S. Shin, "Effect of pre-aging and Al addition on age-hardening and microstructure in Mg-6 wt.%Zn alloys", *Materials Science and Engineering A, 496 (1-2)* (2008) 425 – 433

[15] F.R. Elsayed, T.T. Sasaki, C.L. Mendis, T. Ohkubo, K. Hono, "Significant enhancement of age hardening response in Mg-10Sn-3Al-1Zn alloy by Na microalloying", *Scripta Materialia*, 68 (10) (2013)797-800.